Published in final edited form as:
J Magn Magn Mater. 2010 January 1; 322(2): 190–196. doi:10.1016/j.jmmm.2009.07.086.

Synthesis and characterization of noscapine loaded magnetic polymeric nanoparticles

Mohamed O. Abdalla[1,2], **Ritu Aneja**[3], **Derrick Dean**[4], **Vijay Rangari**[5], **Albert Russell**[6], **Jessie Jaynes**[7], **Clayton Yates**[1,2], and **Timothy Turner**[1,2,*]

[1]Department of Biology, Tuskegee University

[2]Center for Cancer Research, Tuskegee University

[3]Department of Biology, Georgia State University

[4]Department of Materials Science and Engineering, University of Alabama at Birmingham

[5]Tuskegee-Center for Advanced Materials, Tuskegee University

[6]Department of Chemistry, Tuskegee University

[7]George Washington Carver Agricultural Experiment Station, Tuskegee University

Abstract

The delivery of noscapine therapies directly to the site of the tumor would ultimately allow higher concentrations of the drug to be delivered, and prolong circulation time *in vivo* to enhance the therapeutic outcome of this drug. Therefore, we sought to design magnetic based polymeric nanoparticles for the site directed delivery of noscapine to invasive tumors. We synthesized Fe_3O_4 nanoparticles with an average size of 10 ± 2.5 nm. These Fe_3O_4 NPs were used to prepare noscapine loaded magnetic polymeric nanoparticles (NMNP) with an average size of 252 ± 6.3 nm. Fourier transform infrared (FT-IR) spectroscopy showed the encapsulation of noscapine on the surface of the polymer matrix. The encapsulation of the Fe_3O_4 NPs on the surface of the polymer was confirmed by elemental analysis. We studied the drug loading efficiency of polylactide acid (PLLA) and poly (L-lactide acid-co-gylocolide) (PLGA) polymeric systems of various molecular weights. Our findings revealed that the molecular weight of the polymer plays a crucial role in the capacity of the drug loading on the polymer surface. Using a constant amount of polymer and Fe_3O_4 NPs, both PLLA and PLGA at lower molecule weights showed higher loading efficiencies for the drug on their surfaces.

Keywords

noscapine; magnetite; magnetic polymeric nanoparticles

1. Introduction

The current challenges associated with systemic drug administration include even biodistribution of pharmaceuticals throughout the body, lack of drug specificity towards a pathological site, necessity of a large dose to achieve high local concentration, non-specific

*Address correspondence Department of Biology and Center for Cancer Research, Tuskegee University, 100 Carver Research Foundation, Tuskegee, Alabama 36088. turner@tuskegee.edu, Phone (334) 727-8787..

PACS: 42.62.Be, 73.61.Ph, 73.61.Tm

toxicity and adverse side effects due to high drug doses. Chemotherapy induced side effects caused by some current chemotherapy drugs can be so severe that can lead to cessation of the treatment plan for the patient. Therefore, development of drug-systems that could selectively deliver drug molecules to the tumor site, without a concurrent increase in its level in the normal healthy cells of the tissues, is currently one of the most active areas of investigation in cancer research. Among the current attractive schemes of drug targeting, a promising one employs magnetic guided nanoparticles [1;2;3;4;5;6;7]. This technology is based on the encapsulation of drug with magnetic nanoparticles or magnetic nanoparticles coupled to a polymeric carrier. The potential advantage with magnetically guided drug nanoparticles is that the strength of the magnetic field enables the nanoparticles to escape uptake by the reticular endothelial system and multiple drug resistance pumps which are common factors for poor drug performance. Therefore, in recent years the scientific community has been seeking to exploit the intrinsic properties of magnetic nanoparticles to obtain medical breakthroughs in both drug delivery and diagnosis, with emphasis on applications related to cancer [8;9;10;11;12]. Nanoparticles can act at the tissue or cellular level. The latter implies that they can be endocytosed or phagocytosed (i.e. by dendritic cells, macrophages) resulting in internalization of the nanoparticles. In this process, the nanoparticles can reach beyond the cytoplasmatic membrane and, in some cases, also beyond the nuclear membrane (i.e. transfection applications). Tumor targeting with magnetic nanoparticles may use passive or active strategies. Passive targeting occurs as a result of extravasation of the nanoparticles at the diseased site (tumor) where the microvasculature is hyperpermeable and leaky, a process aided by tumor-limited lymphatic drainage. Combined, these factors lead to the selective accumulation of nanoparticles in tumor tissue, a phenomenon known as enhanced permeation and retention (EPR) [10].

Another major advantage of using magnetic particles coupled to a biodegradable polymeric carrier is that the therapeutic drug concentrations are maintained for sustained periods of time. The polymeric matrix prevents drug degradation and also allows precise control over the release kinetics of the drug from the nanoparticles. Moreover, the duration of drug levels released from the nanoparticles can be easily modulated by altering formulation parameters such as drug: polymer ratio, or polymer molecular weight and composition [6;7;13;14;[15];[16];17;18;19;20]. Superparamagnetic iron oxide nanoparticles (Fe_3O_4 NPs) which are commonly used to confer the magnetic property to any polymeric drug delivery systems are also used as popular contrast agents for clinical diagnostics with magnetic resonance imaging (MRI) [21;22]. Therefore, most magnetic drug delivery systems supersede other targeted drug delivery systems because of their dual property as a drug delivery system and an *in vivo* imaging system.

Noscapine, a phthalideisoquinoline antitussive alkaloid has been recently discovered for its tubulin-binding anticancer activity (Figure 1) [23;24;25]. Noscapine causes apoptosis in many cell types and has potent antitumor activity against solid murine lymphoid tumors and against human breast and bladder tumors implanted in nude mice [23]. Although noscapine can inhibit tumor growth and cause regression of tumor xenografts to a fair degree in preclinical mice models, a complete obliteration of the disease has not been achieved even on increasing noscapine dosage as high as 600 mg/kg, possibly due to saturation of its uptake by cancer cells.

We hypothesize that creating magnetically-guided noscapine nanoparticles will present a new method for administering this drug with high-targeting efficiency which will significantly increase its therapeutic index. While reports have not conclusively provided a reason for the remnant cancerous mass upon noscapine treatment, it may be attributed to the rapid elimination of the drug and/or its widespread distribution into non targeted organs and tissues. Currently, clinical data (available on pcref.com) reveals that prostate cancer patients who consume off-label noscapine are on a regimen of about 1000 mg/day of the drug to achieve a lowering of PSA (prostate specific antigen) levels. Although no detectable toxicity has been so far reported

with such enormously high doses of noscapine, consuming such large quantities of drug can present long-term side effects due to accumulation in healthy tissues.

Thus, this system will ensure the delivery of a concentrated dose of noscapine directly into the tumor, which will possibly eliminate the need for the patient to consume large quantities of the drug. This system will have tremendous positive impacts, both physiological and economical on cancer patients. Another advantage of this system is the possibility to use MRI to visualize drug-loaded nanoparticles distribution in the tumor and its surrounding healthy tissues. This is very important because it leads to the next advantages such as: (i) pre-imaging of the drug-free nanoparticles distribution (a tracer dose) to enable a further good prediction of tumor targeting [26], (ii) monitoring during and after administration of the drug-loaded nanoparticles leading to more efficacious treatment [27].

We present here the synthesis and characterization of noscapine loaded magnetic polymeric nanoparticles using two polymeric systems [poly (L-lactide) and poly (DL-lactide-co-glycolide)] and also evaluate the efficiency of the drug loading on these polymers.

2. Experimental

Materials

Benzyl ether, 1,2-hexadecanediol, oleic acid, oleylamine, iron (III) acetylacetonate, poly (L-lactide) with variable average molecular weights [M_w = 100,000-150,000; and 55,000, labeled PLLA-HMW and PLLA-LMW, respectively], poly (DL-lactide-co-glycolide) (PLGA, lactide:glycolide 50:50) [M_w = 40,000-75,000 and 10,000-15,000, labeled PLGA-HMW and PLGA-LMW, respectively], polyvinyl alcohol (PVA) [Mw = 9,000-10,000, 80% hydrolyzed] were all purchased from Sigma Aldrich and stored as specified. All solvents used (hexane, ethanol (200 proof), dichloromethane, acetonitrile, ammonium acetate, water) were HPLC grade and were purchased from Sigma Aldrich Co.

Synthesis of magnetite

Oleic acid-stabilized Fe_3O_4 magnetic nanoparticles were prepared via a high temperature reaction of iron acetylacetonate in phenyl ether in the presence of alcohol, oleic acid and oleylamine according to a reported method [28].

Synthesis of noscapine loaded magnetic nanoparticles

The Fe_3O_4-containing polymeric nanoparticles were prepared by the solvent evaporation/extraction technique in o/w emulsion with PLLA or PLGA as the encapsulation material. 100 mg of PLLA-HMW, 15 mg of Fe_3O_4 NPs and variable amounts of noscapine (2.5, 5, 7.5, 10, 12.5 mg) were dissolved in 8 ml dichloromethane and vortexed for 10 min to make the organic phase. The amount of iron oxide which was used in the formulation was suggested by the literature [11] as the optimum amount to avoid the competition between the iron oxide and noscapine on the surface of the polymer. The organic phase was added to 12 ml of stirred aqueous solution containing 1% PVA as emulsifier. The mixture was sonicated for 120 s with an ultrasonic processor (Sonics, VCX 130 PB). The formed o/w emulsion was then stirred at room temperature overnight with a magnetic stirrer to evaporate the organic solvent. The NMNP were collected by centrifugation at 10,000 rpm for 10 min and washed three times with DI water. The nanoparticles were resuspended with 10 ml water and freeze-dried (Edwards freeze dryer, ESM 1342) for 2 days. The amount of noscapine was varied to quantify the maximum loading of the drug on the polymeric matrix. Based on the results from the above experiment, the encapsulation method was repeated using only 7.5 mg of noscapine with 100 mg of PLLA-LMW, PLGA-LMW, and PLGA-HMW.

Characterization of magnetite and the NMNP

Particle size and surface properties—The synthesized Fe_3O_4 NPs were characterized by X-ray diffraction (Rigaku D/MAX2000, Houston, TX). The XRD samples were prepared by dispersing the synthesized Fe_3O_4 NPs in hexane using an ultrasound sonicator and immediately depositing the sample on a glass holder. After the hexane evaporated, the sample was scanned from 2 to 80 °C. The size of the Fe_3O_4 NPs was estimated from their transmission electronic microscopy (TEM) micrographs using the National Institutes of Health (NIH) ImageJ analysis software. TEM was also used to perform elemental analysis on these nanoparticles. The hydrodynamic size and size distribution of the Fe_3O_4 NPs were determined by dynamic light scattering (DLS) method (Zetasizer nano ZS, Malvern Instruments, Malvern, United Kingdom). TheFe_3O_4 NPs were suspended in deionized (DI) water and sonicated for 10 min to form a uniform dispersion; the DLS analysis was done at 25°C and at a 90°-detection angle. TEM was also used to estimate the size and morphology of the prepared NMNP while DLS was used to determine their hydrodynamic size and size distribution. Zeta potential measurements (Zetasizer nano ZS, Malvern Instruments, Malvern, United Kingdom) were done to determine the surface properties of NMNP. For particle size and surface charge measurements, the mean value of 5 readings was reported. Fourier transform infrared (FT-IR) spectroscopy was used to characterize the encapsulation of noscapine on the surface of the NMNP. The mid-IR spectra were recorded in the range between 650 and 4000 cm^{-1} from 20 scans at a resolution of 4 cm^{-1} using a portable diamond ATR/FT-IR spectrometer (ThermoNicolet model Nexus 470 FTIR spectrometer, Waltham, MA) equipped with an attenuated total reflection (ATR) accessory). Measurements of magnetization of the Fe_3O_4 and NMNP were carried out with a Vibrating Sample Magnetometer (VSM, DMS 1600).

Noscapine encapsulation efficiency—The amount of noscapine incorporated in the nanoparticles produced was determined by high performance liquid chromatography (HPLC) assay. A known amount of the nanoparticles (3 mg) were placed in 5 mL of acetonitrile and left on a shaker overnight. The solution was filtered through a 0.45 μm membrane filter before analysis by HPLC assay using an Agilent 1100 HPLC system. A reverse phase C8 symmetry column (Symmetry C_8, 5 μm, Waters) was used as the stationary phase and the mobile phase used was a mixture of 20 μM ammonium acetate solution and acetonitrile (65:35). The injection volume was 10 μL and the flow rate of the mobile phase was 1 ml/min. The column effluent was monitored at 232 nm with a UV detector. The amount of noscapine in the nanoparticles was determined from the calibration curve of the drug in acetonitrile. The encapsulation efficiency of the drug was calculated as the mass ratio of the amount of the drug entrapped in nanoparticles to that used in the nanoparticles preparation.

3. RESULTS

Synthesis of magnetite

Particle size plays a major role in the degree of magnetism of the material and thus the uniformity of response to external magnetic induction. Therefore, we utilized a synthesis protocol that yielded magnetite nanoparticles with a narrow size distribution (within 10%) to ensure that they will provide a uniform magnetic environment to efficiently direct the nanoparticles [28]. We studied the chemical structure of prepared magnetite by X-ray diffraction. Our results show that the prepared magnetite nanoparticles have six diffraction peaks at 2θ = 29.99, 35.4, 43, 57, 62.5 (degrees) which correlate well with the characteristics peaks of standard Fe_3O_4 crystal (isometric hexoctaheral crystal pattern) (Figure 2) [28]. Figure 3 presents the graph of elemental analysis performed on the prepared Fe_3O_4 which confirmed that the two main elements present on the sample are Fe and O. Elemental analysis detected traces of copper element which was attributed to the TEM copper grid and carbon element was detected due to hexane residues on the surface of the prepared Fe_3O_4.

The size of the prepared Fe_3O_4 NPs was estimated from their TEM micrographs at different magnifications (Figure 4 (a) and (b)). Figure 4 (a) illustrates that the particles have uniform size of about 10 nm (estimated using National Institutes of Health (NIH) ImageJ software), which is comparable to the value reported in the literature [28]. The larger particles observed in the micrographs are simply aggregates of particles because at higher magnification the lattice structures of the separate particles can clearly be identified. The aggregations of these nanoparticles are expected because of their very small size and magnetic property. The estimated size and size distribution of the prepared Fe_3O_4 NPs was confirmed from the DLS data (Table 1).

It is well known that Fe_3O_4 NPs with size less than 30 nm exhibit superparagnatism [10], which is a desirable property in all magnetic drug delivery systems to avoid magnetic agglomeration once the magnetic field is removed. We studied the magnetic property of the synthesized Fe_3O_4 NPs using a Vibrating Sample Magnetometer (VSM, DMS 1600) (see Figure 5 (a)). This curve represents a typical characteristic of superparamagnetic material with no detected remainance or coercivity detected at room temperature. The saturation magnetization (σ_s) of magnetite was 55 which is typical value reported in the literature for this material [28]. Figure 5 (b) shows that no remainance or coercivity was observed with the NMNP, which further confirmed that the single-domain magnetite nanoparticles remain separated in the PLLA matrix. The saturation magnetization value is approximately at a value of 1 for the NMNP prepared with 100 mg PLLA, 15 mg of Fe_3O_4 nanoparticles and 7.5 mg of noscapine.

Synthesis of noscapine loaded magnetic nanoparticles (NMNP)

We prepared NMNP samples using the emulsification-evaporation method using 100 mg as the polymeric carrier, 15 mg of the magnetite and 2.5, 5.0, 7.5, 10.0 and 12.5 mg of noscapine. The particles were labeled NMNP-2.5, NMNP-5.0, NMNP-7.5, NMNP-10, and NMNP-12.5 with the suffix numbers present the amount of noscapine used in the formulation. The prepared nanoparticles were characterized by TEM (Figure 5) to obtain information about the morphology and particle size of the particles). The particles were spherical in shape with an average size of about 250 nm. Elemental analysis obtained from the TEM showed the adsorbed iron oxide nanoparticles on the surface of the polymeric carrier (data not shown).

With the aim to analyze the prepared NPs, FT-IR spectra of pure noscapine, pure PLLA and the prepared NMNP were obtained (see Figure 8). In the fingerprint region range between 700 and 1500 cm^{-1}, noscapine's spectrum (Figure 8 (a)) show numerous sharp bands which are mainly assigned to deformation and stretching vibrations of the alkaloid ring system. Noscapine also show strong band at 1759 which can be described at the C=O stretching vibration, while the –C–O–C– stretching modes can be found at the 1029 cm^{-1} [29]. The spectrum of PLLA (Figure 8 (b)) displays characteristic absorptions C=O stretching at 1756 cm^{-1} and C–O stretch at 1000-1300 cm^{-1}. Figure 8 (c) shows the spectrum of NMNP with the noscapine's spectrum subtracted from it. In figure 8 (c), PLLA sharp bands are observed at C–O stretch 1000-1300 cm^{-1} and C=O stretching at 1756 cm^{-1}. Along with the PLLA sharp bands, figure 8 (c) shows all the characteristic bands for noscapine (noscapine characteristic bands are mostly shown in transmission bands due to subtraction between NMNP and noscapine spectra). We observed in figure 8 (c), noscapine's aromatic vibrational and stretching between 700 and 1000 cm^{-1}, and the –C–O–C– stretching band can be found as a small shoulder at 970-1000 cm^{-1}. As expected, the absorptions for noscapine in NMNP are weaker since the weight percent ratio of the polymer to the drug is 14:1. The presence of the characteristic bands for noscapine and PLLA in the spectrum of the final nanoparticle complex (NMNP) confirmed successful inclusion of noscapine in the polymer system. Figure 8 presents the elemental analysis of the NMNP where the presence of the elements Fe and O on the surface of the NMNP confirmed that the Fe_3O_4 NPs have been encapsulated on the surface of the polymer.

Drug loading efficiency on polymers

Table 1 shows the results from the drug encapsulation procedure using 100 mg PLLA-HMW, 15 mg of iron oxide nanoparticles and various amounts of noscapine. Entrapped noscapine on PLLA-HMW was measured at 1.23, 2.35, 9.5, 9.86, and 12.5% utilizing 2.5, 5, 7.5, 10, and 12.5 mg of noscapine, respectively. These results showed that the compatibility of noscapine with the 100mg of PLLA-HMW is maximal at a starting drug concentration not to exceed 7.5 mg of noscapine. This conclusion was supported from our observation of free noscapine residuals as white powder in the prepared nanoparticles when 10 and 12.5 mg of the drug was used as starting amount of drug in the encapsulation process. Nonetheless, the 7.5 mg of noscapine utilized; resulted in about 0.75 mg of drug encapsulation in the PLLA-HMW matrix. Therefore, the encapsulation process was repeated using a low molecular weight PLLA which showed a drug loading of 19% suggesting that there is a favorite interaction between the abundant free carboxylic groups of the short chain PLLA with the methoxy groups in the noscapine structure. The same trend was observed for the PLGA polymer as an improved drug loading efficiency was observed for the PLGA-LMW at 48% compared to 21 % for the PLGA-HMW (Table 2). This finding with the PLGA strengthened for us our suggestion about the favorable interaction between the carboxylic groups of the short chain polymer with the methoxy groups of the noscapine.

4. Conclusion

We have successfully synthesized and characterized noscapine containing magnetic polymeric nanoparticles using iron oxide nanoparticles, and two FDA approved polymeric systems-PLLA and PLGA. The average size of our prepared NMNP was about 250 nm which is well within the acceptable range for the solvent evaporation/extraction technique in o/w emulsion method. FTIR spectra of PLLA, noscapine, and NMNP showed the encapsulation of the drug on the polymer surface while elemental analysis confirmed the presence of the Fe_3O_4 NPs on the surface of the prepared NMNP. The drug loading efficiency of the drug on the two polymeric systems was studied using HPLC and the drug entrapment was always higher in the case of PLLA or PLGA with the lower molecular weights. Higher values of noscapine entrapment on the low molecular weight polymer were attributed to the favorable interaction between the noscapine methoxy groups and the higher number of free functional groups in the low molecular weight PLLA and PLGA. We are currently studying the *in vitro* and the *in vivo* efficacy of the PLGA system comparing its effectiveness to that of the free drug.

Acknowledgments

The project described was supported by Grant Numbers 3P20MD000195 (NIH/NCMHD), U54 CA118623 (NIH/NCI), and 2G12RR03059 (NIH/RCMI). The content is solely the responsibility of the authors and does not necessarily represent the official views of the National Cancer Institute (NCI), National Center on Minority Health and Health Disparities (NCMHD), Research Centers in Minority Institutions (RCMI) or the National Institutes of Health (NIH).

The authors would like to express their gratitude to Dr. David Nickles from Department of Chemistry, University of Alabama for his assistance with acquiring and analyzing the magnetization data of the iron oxide nanoparticles.

References

[1]. Alexiou C, Arnold W, Klein RJ, Parak FG, Hulin P, Bergemann C, Erhardt W, Wagenpfeil S, Lubbe AS. Locoregional Cancer Treatment with Magnetic Drug Targeting. Cancer Research 2000;60:6641–6648. [PubMed: 11118047]

[2]. Lubbe AS, Bergemann C, Brock J, McClure DG. Physiological aspects in magnetic drug-targeting. Journal of Magnetism and Magnetic Materials 1999;194:149–155.

[3]. Lubbe AS, Bergemann C, Riess H, Schriever F, Reichardt P, Possinger K, Matthias M, Dorken B, Herrmann F, Gurtler R, Hohenberger P, Haas N, Sohr R, Sander B, Lemke A-J, Ohlendorf D, Huhnt

W, Huhn D. Clinical Experiences with Magnetic Drug Targeting: A Phase I Study with 4′-Epidoxorubicin in 14 Patients with Advanced Solid Tumors 1996;56:4686–4693.

[4]. Lubbe AS, Bergemann C, Huhnt W, Fricke T, Riess H, Brock JW, Huhn D. Preclinical Experiences with Magnetic Drug Targeting: Tolerance and Efficacy 1996;56:4694–4701.

[5]. Widder KJ, Senyei AE, Ranney DF. Magnetically responsive microspheres and other carriers for the biophysical targeting of antitumor agents. Advances in Pharmacology and Chemotherapy 1979;16:213–271. [PubMed: 382799]

[6]. Shaffer C. Nanomedicine transforms drug delivery. Drug Discovery Today 2005;10:1581–1582. [PubMed: 16376810]

[7]. Cheng MM-C, Cuda G, Bunimovich YL, Gaspari M, Heath JR, Hill HD, Mirkin CA, Nijdam AJ, Terracciano R, Thundat T, Ferrari M. Nanotechnologies for biomolecular detection and medical diagnostics. Current Opinion in Chemical Biology 2006;10:11–19. [PubMed: 16418011]

[8]. Novakova AA, Lanchinskaya VY, Volkov AV, Gendler TS, Kiseleva TY, Moskvina MA, Zezin SB. Magnetic properties of polymer nanocomposites containing iron oxide nanoparticles. Journal of Magnetism and Magnetic Materials 2003;258-259:354–357.

[9]. Dandamudi S, Campbell RB. The drug loading, cytotoxicty and tumor vascular targeting characteristics of magnetite in magnetic drug targeting. Biomaterials 2007;28:4673–4683. [PubMed: 17688940]

[10]. Arruebo M, Fenandez-Pacheco R, Ibarra MR, Santamaria J. Magnetic nanoparticles for drug delivery. nanotoday 2007;2:22–32.

[11]. Hu FX, Neoh KG, Kang ET. Synthesis and in vitro anti-cancer evaluation of tamoxifen-loaded magnetite/PLLA composite nanocomposites. Biomaterials 2006;27:5725–5733. [PubMed: 16890989]

[12]. Fonseca C, Simoes S, Gasper R. Paclitaxel-loaded PLGA nanoparticles: preparation, physiochemical characterization, and in vitro anti-tumoral activity. Journal of Controlled Release 2002;83:273–286. [PubMed: 12363453]

[13]. Park K. Nanotechnology: What it can do for drug delivery. Journal of Controlled Release 2007;120:1–3. [PubMed: 17532520]

[14]. Nishiyama N. Nanomedicine: Nanocarriers shape up for long life. Nat Nano 2007;2:203–204.

[15]. Morrow KJ Jr, Bawa R, Wei C. Recent Advances in Basic and Clinical Nanomedicine. Medical Clinics of North America 2007;91:805–843. [PubMed: 17826104]

[16]. Gu FX, Karnik R, Wang AZ, Alexis F, Levy-Nissenbaum E, Hong S, Langer RS, Farokhzad OC. Targeted nanoparticles for cancer therapy. Nano Today 2007;2:14–21.

[17]. Vasir JK, Labhasetwar V. Biodegradable nanoparticles for cytosolic delivery of therapeutics. Advanced Drug Delivery Reviews 2007;59:718–728. [PubMed: 17683826]

[18]. Emerich DF, Thanos CG. The pinpoint promise of nanoparticle-based drug delivery and molecular diagnosis. Biomolecular Engineering 2006;23:171–184. [PubMed: 16843058]

[19]. Couvreur P, Gref R, Andrieux K, Malvy C. Nanotechnologies for drug delivery: Application to cancer and autoimmune diseases. Progress in Solid State Chemistry 2006;34:231–235.

[20]. Moghimi SM, Hunter AC, Murray JC. Nanomedicine: current status and future prospects. FASEB J 2005;19:311–330. [PubMed: 15746175]

[21]. Neuberger T, Schöpf B, Hofmann H, Hofmann M, von Rechenberg B. Superparamagnetic nanoparticles for biomedical applications: Possibilities and limitations of a new drug delivery system. Journal of Magnetism and Magnetic Materials 2005;293:483–496.

[22]. Gupta AK, Gupta M. Synthesis and surface engineering of iron oxide nanoparticles for biomedical applications. Biomaterials 2005;26:3995–4021. [PubMed: 15626447]

[23]. Ye K, Ke Y, Keshava N, Shanks J, Kapp JA, Tekmal RR, Petros J, Joshi HC. Opium alkaloid noscapine is an antitumor agent that arrests metaphase and induces apoptosis in dividing cells. Proceedings of the National Academy of Sciences 1998;95:1601–1606.

[24]. Ke Y, Ye K, Grossniklaus HE, Archer DR, Joshi HC, Kapp JA. Noscapine inhibits tumor growth with little toxicity to normal tissues or inhibition of immune responses. Cancer Immunology, Immunotherapy 2000;49(Numbers 45):217–225.

[25]. Landen JW, Lang R, McMahon SJ, Rusan NM, Yvon A-M, Adams AW, Sorcinelli MD, Campbell R, Bonaccorsi P, Ansel JC, Archer DR, Wadsworth P, Armstrong CA, Joshi HC. Noscapine Alters Microtubule Dynamics in Living Cells and Inhibits the Progression of Melanoma 2002:4109–4114.

[26]. Roullin VG, Deverre JR, Lemaire L, Hindre F, Venier-Julienne MC, Vienet RBJP. Anti-cancer drug diffusion within living rat brain tissue: An experimental study using [3H](6)-5-fluorouracil-loaded PLGA microspheres. European Journal of Pharmaceutics and Biopharmaceutics 2002;53:293–299. [PubMed: 11976017]

[27]. Seppenwoolde, J.F.W.N.L.W.B.S.W.Z.A.D.v.h.S.C.J.G.B. Jan-Henry Internal radiation therapy of liver tumors: Qualitative and quantitative magnetic resonance imaging of the biodistribution of holmium-loaded microspheres in animal models. Magnetic Resonance in Medicine 2005;53:76–84. [PubMed: 15690505]

[28]. Sun S, Zeng H, Robinson DB, Raoux S, Rice PM, Wang SX, Li G. Monodisperse MFe2O4 (M = Fe, Co, Mn) Nanoparticles. J. Am. Chem. Soc 2004;126:273–279. [PubMed: 14709092]

[29]. Schulz H, Baranska M, Quilitzsch R, Schütze W. Determination of alkaloids in capsules, milk and ethanolic extracts of poppy (Papaver somniferum L.) by ATR-FT-IR and FT-Raman spectroscopy. Analyst 2004;129:917–920. [PubMed: 15457323]

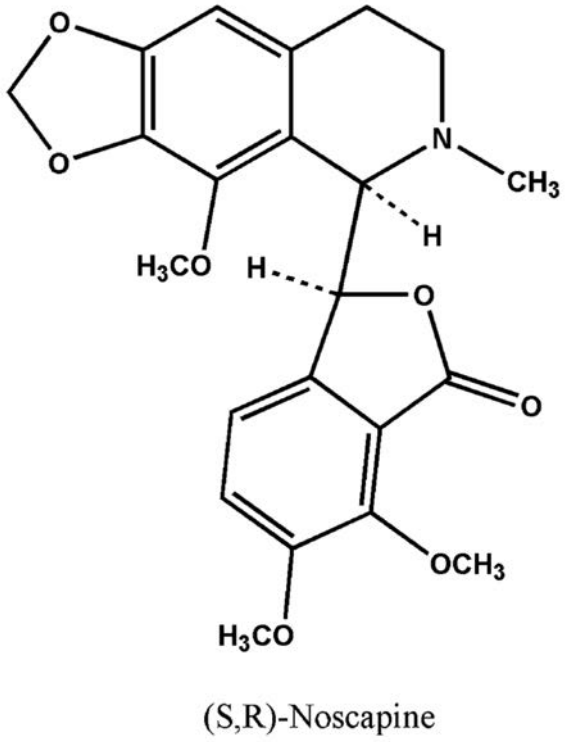

(S,R)-Noscapine

Fig. 1.
Structure of Noscapine

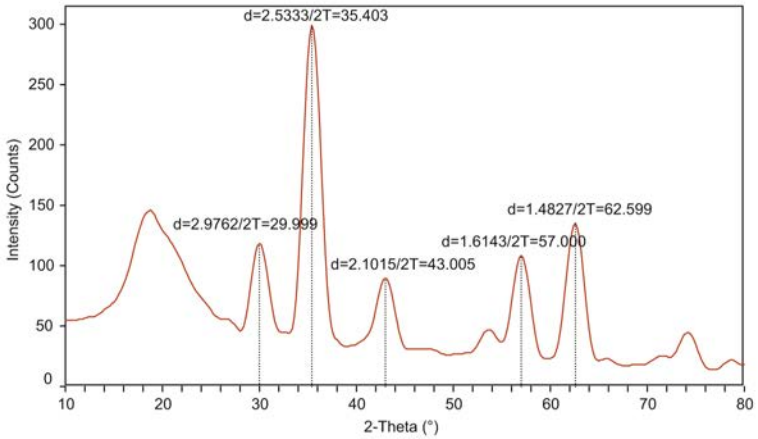

Fig. 2.

XRD pattern of synthesized magnetite shows a typical pattern for Fe_3O_4 NPs crystal structure with six characteristics peaks.

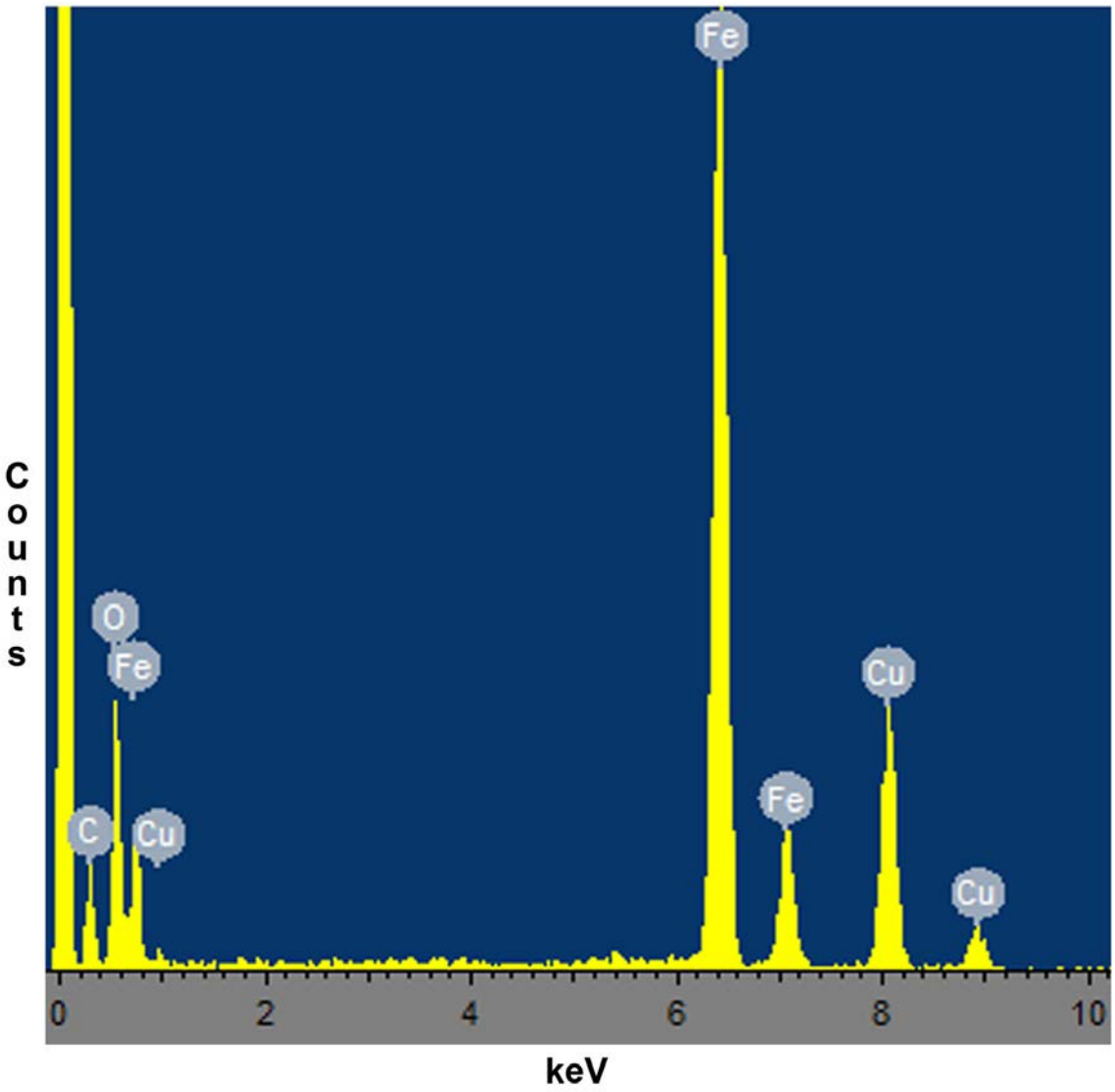

Fig. 3.

Elemental analysis of the Fe_3O_4 NPs which verified that the main elements in the NPs are Fe and O. Copper (Cu) element was detected as the sample holder is made of Cu and Carbon was detected due to the hexane traces on the surface of the Fe_3O_4 NPs.

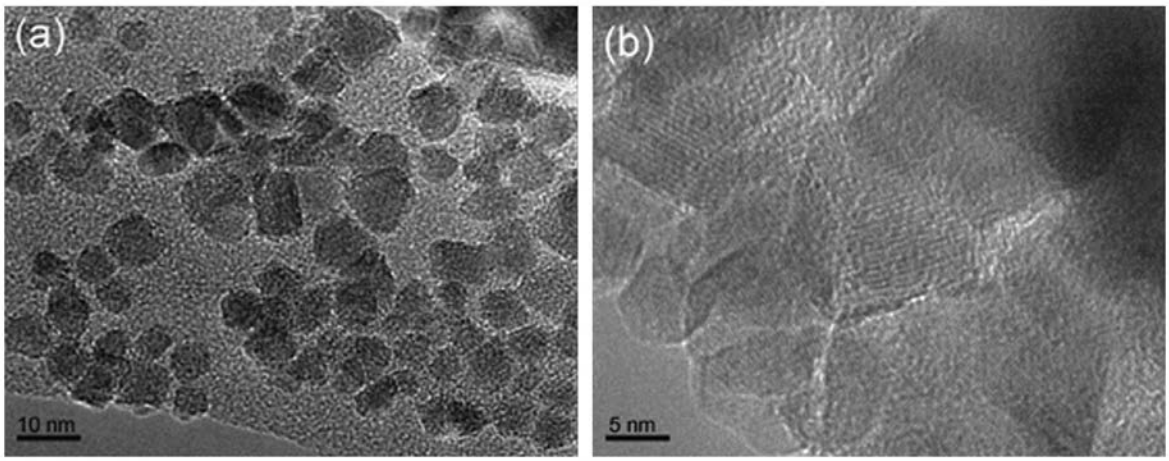

Fig. 4.

TEM micrographs on synthesized magnetite, (a) bar = 10 nm, shows that bulk of the nanoparticles synthesized are of uniform size with few aggregates (b) bar = 5 nm scale, a magnified image of shows that an aggregate is a collection of nanoparticles with different lattice structures.

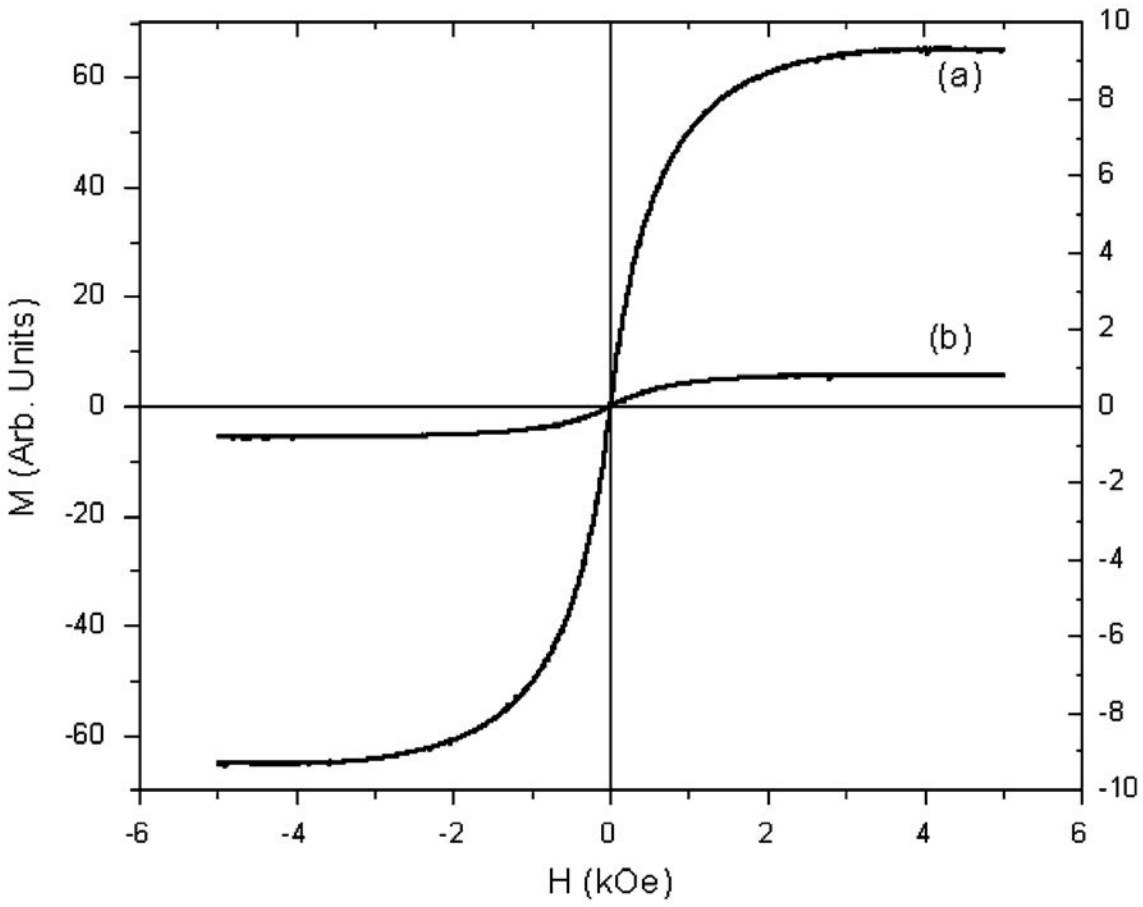

Fig. 5.
Field dependent magnetization at 25°C for (a) Fe_3O_4 NPs and (b) NMNP (prepared with 100 mg PLLA, 15 mg Fe_3O_4 and 7.5 mg noscapine).

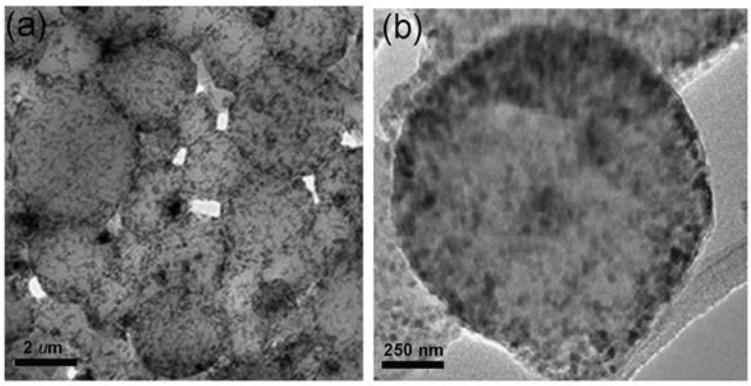

Fig. 6.

TEM micrographs of NMNP prepared with 100 mg PLLA, 15 mg, Fe_3O_4 NPs and 7.5 mg noscapine a) bar = 1.0 um, shows that bulk of the nanoparticles synthesized are of uniform size with few aggregates (b) bar = 50 nm scale, a magnified image of shows a spherical shaped NMNP with an approximate size of 250 nm.

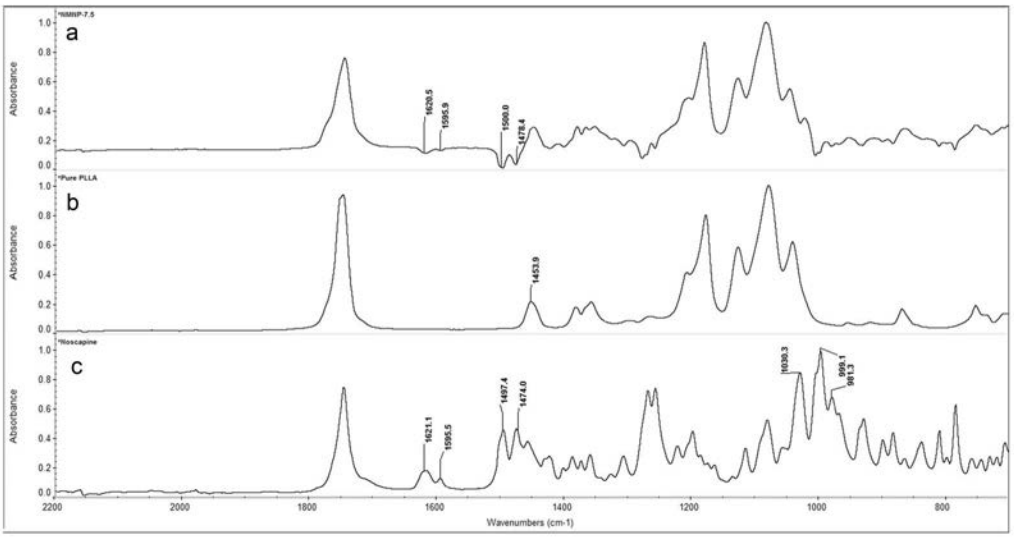

Fig. 7.

Infrared spectrum of (a) noscapine: sharp bands between 700-1500 cm^{-1} which are mainly assigned to deformation and stretching vibrations of the alkaloid ring system and C=O stretch at 1759 cm^{-1}, (b) pure PLLA: C=O stretch 1756 cm^{-1}, C–O stretch 1000-1300 cm^{-1}, (c) NMNP-7.5: absorption bands for both PLLA and noscapine are observed (noscapine's absorption bands are shown in transmittance mode due to subtraction between NMNP and noscapine spectra).

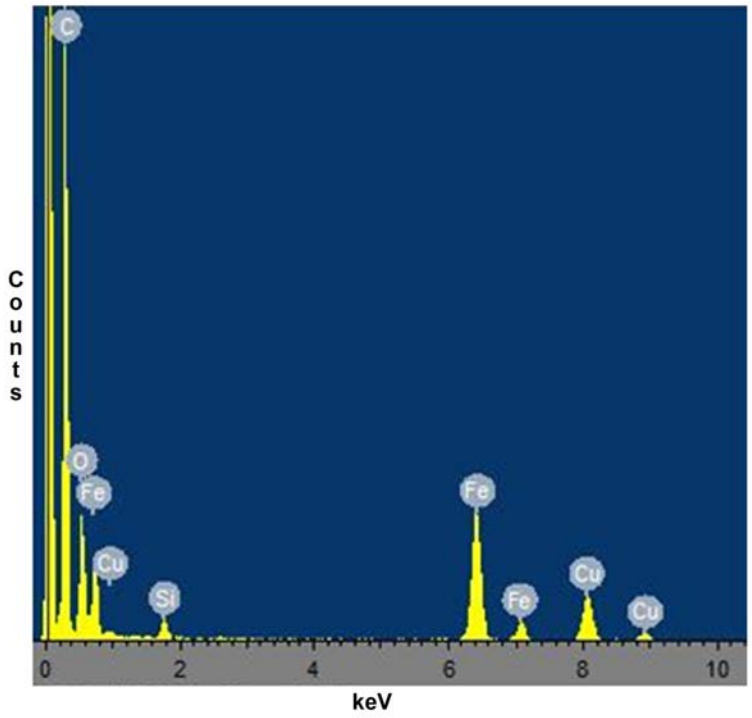

Fig. 8.

Elemental analysis of the NMNP verified the presence of elements Fe and O on the surface of the polymeric nanoparticles which proved the encapsulation of the Fe_3O_4 NPs on the surface of the polymer.

Table 1

Size and zeta potential characterization of prepared Fe_3O_4 NPs and NMNP

Nanoparticles types	Fe_3O_4	NMNP*
Hydrodynamic Size (nm) (TEM)	10 ± 2.5	252 ± 6.3
Hydrodynamic Size (nm)* (DLS)	12.1 ± 5.2	243 ± 23
Zeta Potential (mV)	------	−15.7 ± 2.4

* Prepared with 100 mg of PLLA-HMW, 15 mg Fe_3O_4 NPs,7.5 mg noscapine. Data represents mean ± SD, $n = 3$

Table 2

Noscapine encapsulation data using PLLA-HMW

Sample	NMNP-2.5*	NMNP-5	NMNP-7.5	NMNP-10	NMNP-12.5
% Drug loading	0.9	2.1	9.2	10.1	12.9

*All samples were prepared with 100 mg of PLLA-HMW, 15 mg Fe_3O_4 NPs, suffix presents the amount of noscapine in mg. Data represents mean ± SD, $n = 3$.

Table 3

Noscapine encapsulation data using PLLA-LMW, PLGA-LMW, PLGA-HMW

Sample	PLLA-LMW*	PLGA-HMW	PLGA-LMW
% Drug loading	18.2	22	48

* All samples were prepared using 100 mg of the polymer, 15 mg of iron oxide nanoparticles and 7.5 mg of noscapine. Data represents mean ± SD, n = 3.